



Numerical Investigation of Bond Interface Morphology between Normal Strength Concrete and Ultra-High-Performance Concrete under Shear Loading

Jiebo Fan^a, Mengkai Lin^{b*}, Wen Sun^c

School of Civil Engineering, Lanzhou Jiaotong University, Lanzhou, Gansu, China

^a473572747@qq.com, ^{b*}27834040@qq.com, ^csunwen@lztu.edu.cn

Abstract. In order to address the challenge of accurately quantifying the roughness of the bond interface morphology between Normal Strength Concrete (NSC) and Ultra-High-Performance Concrete (UHPC), this study employed the spatial frequency content method to characterize randomly rough surfaces. The roughness was quantified using the sand filling method, and subsequently, a "Z"-shaped direct shear finite element model with rough bonding surfaces was established. The results indicate that the rough surfaces generated by the spatial frequency content method can be applied to the bonding interfaces of both types of concrete. This approach facilitates the three-dimensional characterization of the bond interface morphology and roughness, yielding reliable simulation results. The failure mode obtained from the finite element model corresponds precisely to the actual observed behavior. Through analysis, it was determined that shear loading is primarily borne by the effective bonded area and mechanical interlocking forces.

Keywords: Ultra-High-Performance Concrete; Surface Morphology; Shear Action; Modeling; Restoration.

1 Introduction

In recent years, the aging issues of concrete structures have become increasingly prominent, necessitating the maintenance and strengthening of concrete structures[1,2]. Through years of practical application, Ultra-High-Performance Concrete (UHPC) has emerged as a crucial choice for concrete reinforcement and repair materials, owing to its exceptional strength, bond performance, durability, ductility, and environmentally sustainable properties[3-5]. However, the repaired bond interface often becomes a weak point for load transfer between concrete elements[3]. To enhance the strength of the repaired bond interface, it is essential to roughen the bonding surface[6]. This is because a rough bonding surface encapsulates the micro-mechanisms and fundamental information of the bond interface, providing a comprehensive reflection of the concrete's microstructure and other influencing factors[7]. It serves as a critical factor in evaluating bonding performance, reinforcement effects, and predicting bond strength

© The Author(s) 2024

P. Liu et al. (eds.), *Proceedings of the 2024 5th International Conference on Civil, Architecture and Disaster Prevention and Control (CADPC 2024)*, Atlantis Highlights in Engineering 31,

https://doi.org/10.2991/978-94-6463-435-8_19

between interfaces. The specific parameters of the bond interface require representation through interfacial roughness. To address the limitations of purely qualitative assessments of interfacial roughness, it becomes imperative to quantitatively describe the roughness of the bond interface[8]. Additionally, existing research on quantifying bond interface roughness is confined to cases where concrete surfaces exhibit smooth morphology[9]. Attention to bond interface roughness has mainly focused on relatively regular interfaces, leaving limited understanding of the bonding performance for rough interfaces closer to real-world conditions. Therefore, quantifying and evaluating roughness as a parameter for studying changes in interfacial bonding capabilities is essential. Faced with these challenges, it becomes crucial to integrate rough bonding surfaces with both types of concrete seamlessly, and quantify the roughness of the bond interface accurately. An effective approach to achieve this is through numerical research. In this study, we adopt the spatial frequency content method to characterize randomly rough surfaces, and then quantitatively assess surface roughness through simulated sand casting. Based on these findings, the rough surface model is applied to the bond interface between UHPC and NC, aiming to study the bond interface morphology between the two types of concrete.

2 Rough bonding surface

Based on the concepts of spatial frequency and fundamental waves, rough surface data are synthesized through the sum of trigonometric functions.

2.1 Characterization of rough surface

Suppose that the shape function of a rough surface is a cosine. The following double summation was used to represent a rough surface[10]:

$$f(x, y) = \sum_{m=-N}^N \sum_{n=-N}^N \omega(m, n) \cos(2\pi(mx + ny) + \phi(m, n)) \quad (1)$$

where, x and y are spatial coordinates; m and n are spatial frequencies; $\omega(m, n)$ is amplitude; $\phi(m, n)$ is the phase angle, N represents the value range of m and n .

2.2 Quantified roughness

The average roughness is expressed as the mean depth of sand filling, which is obtained by dividing the sand-filling volume by the bonding area of the UHPC-NC interface[11].

$$R_m = h = \frac{V}{ab} \quad (2)$$

where h is the average sand-filling depth (mm); a and b are the length and width of the concrete bonding surface, respectively (mm); V is the sand-filling volume (mm³).

2.3 Build a rough surface

The rough surface constructed according to the theoretical description in Sections 1.1 and 1.2 is shown in Fig. 1, and its roughness $R_m=8.54\text{mm}$.

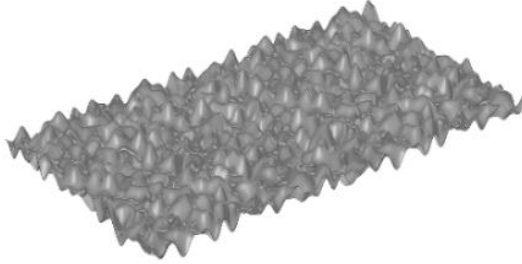


Fig. 1. Rough surface

3 Finite element model

3.1 Model size

This study uses the "Z"-shaped direct shear specimen as a model to study the influence of UHPC-NC bonding surface morphology and roughness on the interface shear characteristics. After design, the rough surface constructed in Section 1.3 is inserted between UHPC and NC, its dimensions are shown in Fig. 2.

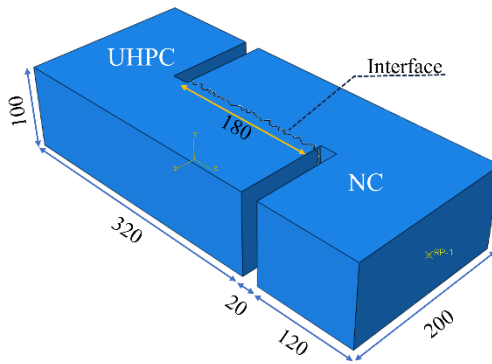


Fig. 2. Specimen size drawing

3.2 Determination of constitutive relations

It employs stress-strain relationships to define material properties of concrete, as illustrated in Fig. 3. The interface constitutive model adopts the traction-separation bilinear constitutive model, as illustrated in Fig. 4[12,13].

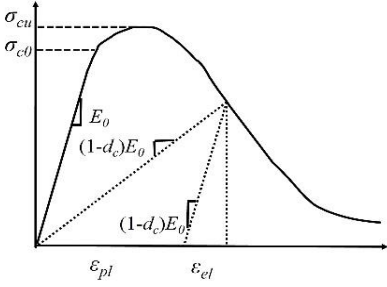


Fig. 3. Stress-strain curve of concrete under uniaxial compression

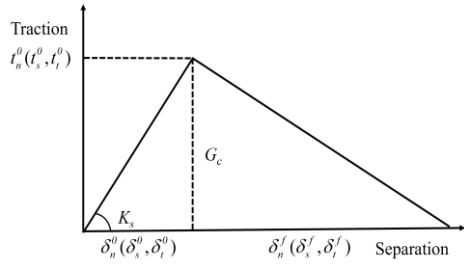


Fig. 4. Traction-separation constitutive model

3.3 Result analysis

Phenomenon analysis.

SDEG (Stiffness Degradation) signifies the decrease in stiffness due to damage. According to numerical simulation results, the post-shear failure morphology of the specimen is illustrated in Fig. 5. It is evident that a portion of the interface bonding in the model exhibits cracking, and concurrent damage occurs in the vicinity of the bonding surface in the Normal Strength Concrete (NC). Some partially peeled-off NC remains bonded to the Ultra-High-Performance Concrete (UHPC). The mechanical interlocking forces provided by the rough bonding surface transform the failure of the UHPC-NC bonding surface into a simultaneous failure of the NC and the interface. This is attributed to the fact that one of the mechanisms through which roughness influences the UHPC-NC bonding surface is by promoting mechanical interlocking forces[3]. Therefore, the finite element calculations align well with the observed real-world scenario.

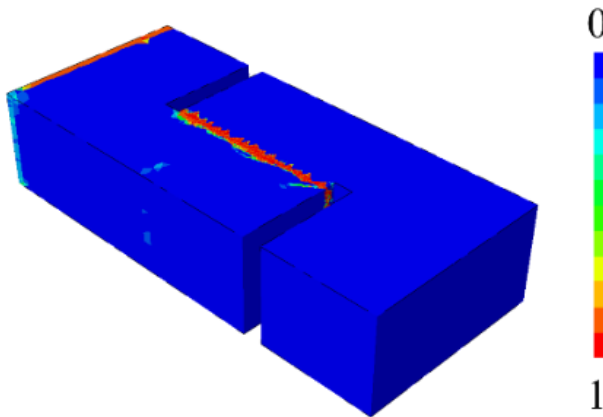


Fig. 5. SEDG cloud chart

Load-slip curve.

Based on the results obtained from finite element calculations, the load-slip curve is plotted, as shown in Fig. 6, and the curve aligns well with real-world observations. The initial phase of the curve exhibits linear growth, reaching a peak where bonding surface damage occurs, and the effective bonded area decreases. Subsequently, the mechanical interlocking forces provided by the rough bonding surface come into play, transferring the interface damage to the NC and initiating the yielding stage. The curve then demonstrates a distinct ductile failure. Through analysis, it is determined that shear loading is predominantly borne by the effective bonded area and mechanical interlocking forces[14].

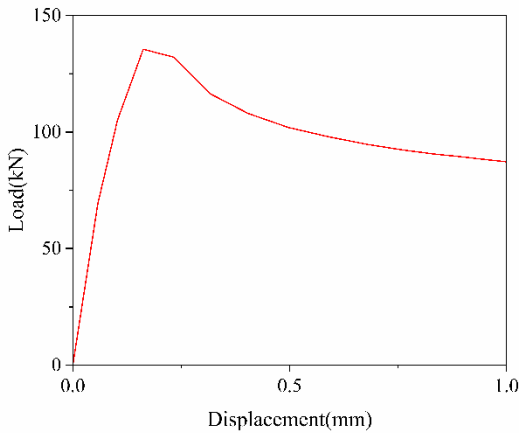


Fig. 6. Load-slip curve

4 Conclusion

(1) The randomly rough surfaces generated using the spatial frequency content method exhibit a uniform distribution of concave-convex features, with minimal localized defects that could introduce discrete effects. This characteristic makes them suitable for application to the bonding interfaces of both types of concrete, allowing for the exploration of three-dimensional morphology and the effects of rough bonding surfaces.

(2) In this study, a "Z"-shaped direct shear model for UHPC-NC was established, incorporating randomly rough surfaces at the bonding interface. Through analysis, the simulated phenomena align with real-world observations, indicating the reliability of the simulation results.

References

1. A. Manawadu, P. Qiao, H. Wen, Characterization of Substrate-to-Overlay Interface Bond in Concrete Repairs: A Review, *Constr. Build. Mater.* 373 (2023) 130828, 10.1016/j.conbuildmat.2023.130828.
2. Y. Wang, X. Jiang, K. Li, J. Qiang, Experimental study of interfacial adhesion performance of prefabricated UHPC-NC diagonal shear groove, *Case Stud. Constr. Mater.* 19 (2023) e2343, 10.1016/j.cscm.2023.e02343.
3. S. Feng, H. Xiao, M. Ma, S. Zhang, Experimental study on bonding behaviour of interface between UHPC and concrete substrate, *Constr. Build. Mater.* 311 (2021) 125360, <https://doi.org/10.1016/j.conbuildmat.2021.125360>.
4. M. Amran, G. Murali, N. Makul, W.C. Tang, A. Eid Alluqmani, Sustainable development of eco-friendly ultra-high performance concrete (UHPC): Cost, carbon emission, and structural ductility, *Constr. Build. Mater.* 398 (2023) 132477, 10.1016/j.conbuildmat.2023.132477.
5. J.A. Mash, K.A. Harries, C. Rogers, Repair of corroded steel bridge girder end regions using steel, concrete, UHPC and GFRP repair systems, *J. Constr. Steel Res.* 207 (2023) 107975, 10.1016/j.jcsr.2023.107975.
6. M.A. Al-Osta, S. Ahmad, M.K. Al-Madani, H.R. Khalid, M. Al-Huri, A. Al-Fakih, Performance of bond strength between ultra-high-performance concrete and concrete substrates (concrete screed and self-compacted concrete): An experimental study, *J. Build. Eng.* 51 (2022) 104291, 10.1016/j.jobe.2022.104291.
7. B.A. Tayeh, B.H. Abu Bakar, M.A. Megat Johari, Characterization of the interfacial bond between old concrete substrate and ultra high performance fiber concrete repair composite, *Mater. Struct.* 46 (5) (2013) 743-753, 10.1617/s11527-012-9931-1.
8. J. Tian, X. Wu, W. Wang, S. Hu, X. Tan, Y. Du, Y. Zheng, C. Sun, Experimental study and mechanics model of ECC-to-concrete bond interface under tensile loading, *Compos. Struct.* 285 (2022) 115203, 10.1016/j.compstruct.2022.115203.
9. M.K. Al-Madani, M.A. Al-Osta, S. Ahmad, H.R. Khalid, M. Al-Huri, Interfacial bond behavior between ultra high performance concrete and normal concrete substrates, *Constr. Build. Mater.* 320 (2022) 126229, 10.1016/j.conbuildmat.2021.126229.
10. J. Wu, Simulation of rough surfaces with FFT, *Tribol. Int.* 33 (1) (2000) 47-58, [https://doi.org/10.1016/S0301-679X\(00\)00016-5](https://doi.org/10.1016/S0301-679X(00)00016-5).
11. Y. Yin, Y. Fan, Influence of Roughness on Shear Bonding Performance of CFRP-Concrete Interface, *Materials.* 11 (10) (2018) 1875, 10.3390/ma11101875.
12. M. Farzad, M. Shafieifar, A. Azizinamini, Experimental and numerical study on bond strength between conventional concrete and Ultra High-Performance Concrete (UHPC), *Eng. Struct.* 186 (2019) 297-305, 10.1016/j.engstruct.2019.02.030.
13. S. Yuan, Z. Liu, T. Tong, Y. Wang, A coupled adhesive-frictional model tailored for interfacial behaviors between UHPC and NC materials, *Structures.* 38 (2022) 1397-1410, 10.1016/j.istruc.2022.02.061.
14. B. Singh Negi, K. Jain, Shear resistant mechanisms in steel fiber reinforced concrete beams: An analytical investigation, *Structures.* 39 (2022) 607-619, 10.1016/j.istruc.2022.03.061.

Open Access This chapter is licensed under the terms of the Creative Commons Attribution-NonCommercial 4.0 International License (<http://creativecommons.org/licenses/by-nc/4.0/>), which permits any noncommercial use, sharing, adaptation, distribution and reproduction in any medium or format, as long as you give appropriate credit to the original author(s) and the source, provide a link to the Creative Commons license and indicate if changes were made.

The images or other third party material in this chapter are included in the chapter's Creative Commons license, unless indicated otherwise in a credit line to the material. If material is not included in the chapter's Creative Commons license and your intended use is not permitted by statutory regulation or exceeds the permitted use, you will need to obtain permission directly from the copyright holder.

